Agr. Nat. Resour. 60 (2026) 600110

AGRICULTURE AND NATURAL RESOURCES

Journal homepage: http://anres.kasetsart.org

Research article

Effect of bambara bean and barley flour inclusion on nutritional, functional, structural and pasting properties of broken rice-based blends

Agus Setiyoko[a,f], Rabiha Sulaiman[a,e,*], Nor Afizah Mustapha[a], Mohd Khairol Anuar Mohd Ariffin[b], Slamet Budijanto[c], Eny Palupi[d]

[a] *Department of Food Technology, Faculty of Food Science and Technology, Universiti Putra Malaysia, 43400 Serdang, Selangor Darul Ehsan, Malaysia*

[b] *Department of Mechanical and Manufacturing Engineering, Faculty of Engineering, Universiti Putra Malaysia, 43400 Serdang, Selangor Darul Ehsan, Malaysia*

[c] *Department of Food Science and Technology, Faculty of Agricultural Engineering and Technology, IPB University, Bogor 16680, Indonesia*

[d] *Department of Community Nutrition, Faculty of Human Ecology, IPB University, Bogor 16680, Indonesia*

[e] *Halal Products Research Institute, Universiti Putra Malaysia, 43400 Serdang, Selangor Darul Ehsan, Malaysia*

[f] *Department of Agricultural Product Technology, Faculty of Agroindustry, Universitas Mercu Buana Yogyakarta, Yogyakarta 55753, Indonesia*

Article Info

Article history:
Received 26 August 2025
Revised 14 December 2026
Accepted 19 January 2026
Available online 28 February 2026

Keywords:
Bambara bean,
Broken rice,
Flour blends,
Functional properties,
Pasting properties,
Structural

Abstract

Importance of the work: A novel triple-flour blend was developed by mixing underutilized broken rice with barley and bambara bean flour a combination remains to be studied, with other published research focusing mainly on each component individually.

Objectives: To investigate the nutritional composition, structural properties, pasting characteristics and functional properties of composite flours.

Materials and Methods: Composite flours with varying ratios of broken rice, barley and bambara bean were analyzed for proximate composition, antioxidant activity, functional properties, pasting behavior, Fourier-transform infrared (FTIR) spectra and X-ray diffraction patterns.

Results: Increasing the bambara bean flour content significantly enhanced the protein, fiber, fat and antioxidant levels, while reducing the starch and amylose contents. The water absorption index increased with higher inclusion of bambara beans and barley. All blends exhibited A-type crystallinity; however, crystallinity decreased in the high-bambara formulations, indicating an increase in amorphous structures. Reduced setback viscosity was suggested to improve thermal stability and resistance to retrogradation. FTIR spectroscopy confirmed the presence of similar functional groups, with intensity differences reflecting compositional variation. Antioxidant activity increased significantly in the bambara-rich blends.

Main finding: These blends offer enhanced nutritional value, functional quality and structural characteristics, highlighting their potential for functional and sustainable food applications.

* Corresponding author.
E-mail address: rabiha@upm.edu.my (R. Sulaiman)

https://doi.org/10.34044/j.anres.2026.60.1.10

Introduction

Broken rice (*Oryza sativa* L.) is a by-product of rice that can be processed into flour and may consist of one or multiple size fractions, depending on the milling method (Tan and Norhaizan, 2020). Milling losses in rice and pulse mills are in the range 1520% (Nisha et al., 2023). Despite physical damage, broken rice retains its nutritional value (Nisha et al., 2023), making it a cost-effective ingredient. Rice flour has a mild flavor and is colorless, hypoallergenic, low in salt and easily digestible (Ren et al., 2020; Hasmadi & Ronie, 2022). Currently, these broken rice and pulse mill by-products are applied in ready-to-use mixes and biscuits, serving as a corn alternative in buffalo diets and a maize substitute in broiler diets (Jozinović et al., 2021). The current study utilized broken rice, barley and bambara beans as basic materials. The selection of these raw materials was based on broken rice being an underutilized milling by-product with potential for value enhancement. Barley and bambara bean were included for their rich dietary fiber, protein and bioactive components, which could improve the quality of composite flour compositions. This combination offers sustainability advantages using by-products and enhances nutrition through cereal-legume enrichment.

Barley (*Hordeum vulgare* L.) is acknowledged as a nutraceutical grain because of its bioactive compounds, which include β-glucan, phenolic compounds, B-complex vitamins, tocotrienols and tocopherols (Zeng et al., 2020). This cereal has greater antioxidant activity than commonly consumed grains, such as wheat and rice, effectively reducing blood cholesterol levels and the glycemic index, thereby contributing to the prevention of cardiovascular disease (Lukinac and Jukić, 2022). Whole grain barley consists of 57.760.7% carbohydrate, 2.52.7% fat, 12.215.1% protein, 16.620.6% dietary fiber, 4.85.7% β-glucan, 1.21.5% sugar and 1.62.1% ash, contingent upon whether the grain type is hulled or dehulled (Lukinac and Jukić, 2022; Kaur et al., 2024).

Bambara bean (*Vigna subterranean* L.) is an utilized legume rich in essential nutrients, including carbohydrate (53–69%), oils (6–8.5%), protein (18–24%), minerals (2.5–3.5%) and total dietary fiber 10.3%, with tryptophan as the limiting amino acid (Ogundele et al., 2017). It contains low soluble fiber, 1.4% fat and a high proportion of unsaturated fatty acids (61%), particularly n-6 fatty acids (36%). Phosphorus is the dominant mineral, with magnesium, calcium and trace elements such as iron, copper and zinc also present (Yao et al., 2015). The bean is rich in polyphenols, including flavonoids (quinic, chlorogenic, caffeic and ellagic acids), which provide health benefits and enhance immune response (Okafor et al., 2022). Its antioxidant properties help to reduce lipid oxidation and limit metal ion-oxygen interactions in food (Oyeyinka et al., 2021).

Blending is the process of combining ingredients to create a homogeneous product, commonly used in food production to enhance functional attributes and nutrient content (Liu et al., 2024). Substituting 20-30% of wheat flour with barley flour in bread and pasta enhances the nutritional value without significantly affecting sensory attributes (Lukinac and Jukić, 2022). A blend of 15% bambara groundnut flour and 85% purple sweet potato flour produced a product with a higher fiber content and shorter cooking time than commercial analogs (Ariyantoro et al., 2021).

The characteristics of food ingredients significantly influence the processing properties of final products (Liu et al., 2024). A blend of broken rice, barley and Bambara bean flour can be used to produce a variety of rice-based products; combining these flours in different ratios can enhance nutritional value while maintaining desirable sensory qualities. Therefore, it is essential to assess the properties of such blends. Consequently, the current examined the nutrient composition, functional properties, structural characteristics and pasting attributes of composite flours produced by varying the ratio of broken rice, barley and bambara bean flour. The results should contribute to global food security by promoting food diversification using underutilized crops.

Materials and Methods

Materials

Broken rice (*Oryza sativa* L.) (KM 0199) grains harvested in May 2024 were obtained from the BERNAS Rice Milling Plant at Seri Tiram Jaya, Tanjung Karang, Selangor, Malaysia. Barley grains (*Hordeum vulgare* L.; KM 0200, Double Swallow brand) were obtained from the local market in Putrajaya, Malaysia. The black-skinned bambara beans (*Vigna subterranea* (L.) Verdc.), locally known as kacang bogor (KM 0183), harvested in April 2024, were obtained from Jampang Kulon District, Sukabumi Regency, West Java Province, Indonesia.

Composite flour preparation

The raw components were ground into flour utilizing a DF-25 (China) grinder machine featuring a 0.50 mm sieve mesh. The flour samples were contained in polyethylene bags, vacuum-sealed and stored at 4°C until subsequent examination. The flour blends were prepared by manually mixing broken rice, barley and bambara bean flour according to the predetermined ratios (Table 1) using a stainless-steel hand whisk for 5 min, until a homogeneous mixture was obtained. A screening-based fixed-ratio design was used to determine seven formulations. The design consisted of three single-component flours (100% broken rice, 100% barley, 100% Bambara bean) as baseline controls, three balanced binary blends (50:50) to examine the co-effects between the two components and one ternary mixture (50:25:25) to investigate the first three-component interactions. The ratios were selected based on the nutritional complementarity and functional compatibility of the components. This method was selected for its efficiency and practicality for evaluating the impacts of individual and combination components on the characteristics of composite flours, without necessitating a complete mixture design, which could be used for further research. The composite flour formulations were uniformly blended into seven different formulations, as detailed in Table 1.

Table 1 Sample codes and flour compositions of the formulated blends containing broken rice flour, barley flour, and bambara bean flour.

Sample code	Composition
F1	100% Broken rice flour
F2	100% Barley flour
F3	100% Bambara bean flour
F4	50% Broken rice flour: 50% Barley flour
F5	50% Broken rice flour: 50% Bambara bean flour
F6	50% Barley flour: 50% Bambara bean flour
F7	50% Broken rice flour: 25% Barley flour: 25% Bambara bean flour

Analysis of the structural, nutritional and pasting characteristics of blended flours

Compositional analysis

The proximate composition of flours was determined using the method of Horwitz and Latimer (2005), while the method of Thiranusornkij et al. (2019) was used to analyze the amylose content. A 100 mg flour sample was diluted with 1 mL of 95% ethanol and 9 mL of 1 N NaOH, then allowed to stand at room temperature for 10 minutes.

Next, the solution was heated in a water bath at 100°C for 10 min and allowed to cool to room temperature for at least 2 hr. The solution was diluted to a volume of 100 mL and subjected to vigorous vortexing. The sample solution (5 mL) was incubated with 50 mL of distilled water, 2 mL of 1 N acetic acid and 2 mL of iodine solution and afterward diluted to 100 mL with distilled water. Absorbance was recorded at 620 nm following incubation for 20 min. Pure amylose derived from potatoes was utilized to establish a standard curve for quantifying the amylose content. Total starch was quantified in accordance with AOAC 920.44, implemented by Lafont-Mendoza et al. (2018). At the same time, the amylopectin content was determined by subtracting the amylose amount from the total starch (Palupi et al., 2015).

Total dietary fiber (TDF) and soluble dietary fiber (SDF) were measured using an enzymatic-gravimetric method (Megazyme K-TDFR; Ireland). Heat-stable α-amylase (35 min boiling), protease and amyloglucosidase (30 min 60°C) were used to digest 1 g of sample in MesTris buffer. Ethanol was used to precipitate the SDF from the filtrate, which was then filtered, dried at 105°C and adjusted for any remaining ash and protein. Similar methods were used to determine TDF, but using direct precipitation without filtration.

Color

The color characteristics of samples were analyzed using a colorimeter (CR-410; Konica Minolta;Japan) and the Hunter technique based on lightness (L*), greenness (a*) and blueness (b*). A white tile was used to calibrate the apparatus. The whiteness index was calculated using Equation 1 while the hue angle Equation 2 and chroma Equation 3 were computed using the methodology of Nevara et al. (2019):

$$\text{Whiteness index} = 100 - [(100 - L)^2 + a^2 + b^2]^{0.5} \quad (1)$$

$$\text{Hue angle} = \tan^{-1}(b / a) \quad (2)$$

$$\text{Chroma} = \sqrt{a^2 + b^2} \quad (3)$$

Water activity

An AquaLab 3TE meter (METER Group, Inc.; Pullman, WA, USA) was used to measure water activity (a_w). The flour was placed into a reusable cup, thoroughly covering the base prior to the automated measurements being taken.

Particle size

The samples were determined using a laser particle size analyzer (Mastersizer 3000; Malvern Instruments Ltd.; Malvern, UK) equipped with a dry dispersion system, involving the spans (D90-D10/D50), (D50), D10 and D90, a refractive index of 1.53 and a consistent obscuration of 30% in all measurements. All assays were performed in triplicate.

Fourier transform infrared spectroscopy

Fourier transform infrared (FTIR) spectra were obtained by mixing KBr (chromatographic grade) with the sample flour (100 mg), milling it in an agate mortar and pressing it into translucent slices. Samples were scanned 50 times using a Nicolet IS 10-spectrometer (Thermo Fisher Scientific, Co.; Waltham, MA, USA) for the range 4000–400 cm^{-1}. Spectral data were analyzed using the OMNIC version 8.2 and PeakFit version 4.12 software packages (Lv et al., 2022).

Pasting properties

The pasting properties were measured using a Rapid Visco Analyzer (RVA) 4500 (Newport Scientific; Avon, MN, USA) on 3 g of rice flour (14% moisture content) in 25 mL of distilled water. The sample was heated from ambient temperature to 95°C (12°C/min), held for 23 min and then cooled to 50°C (12°C/min), during a total of 13 min. Parameters recorded were: peak viscosity, trough, breakdown, final viscosity, setback, peak time and pasting temperature (Thiranusornkij et al., 2019).

X-ray diffraction

The X-ray diffraction (XRD) analysis was performed using an AXS D8 Discover diffractometer (Bruker Corp.; Billerica, MA, USA), with a copper source, 40 kV and 45 mA over a range of 5 -40° 2θ at 0.02°/s. Relative crystallinity was calculated as the ratio of crystalline peak area to total diffraction area. Complementary FTIR spectra were collected within the spectral range 4000 – 400 cm^{-1}.

Functional properties

Water absorption index

The water absorption index (WAI), measured in grams per gram, was evaluated using the methodology outlined by Kharat et al. (2019) and based on Equation 4:

$$\text{Water absorption index (g/g)} = \text{Sediment wet weight} / \text{Sediment dry weight} \quad (4)$$

where all weights are in grams.

Water solubility index and swelling power

The water solubility index (WSI) as a percentage and the swelling power measured in grams per gram were evaluated following the methods specified by Mustapha et al. (2024) and using Equation 5 and Equation 6:

$$\text{Water solubility index} = \frac{\text{Weight of dried supernatant}}{\text{Weight of dry sample}} \quad (5)$$

$$\text{Swelling power} = \frac{\text{Wet sediment weight}}{\text{Dry flour sample weight} \times (100 - \text{WSI})} \quad (6)$$

where all weights are in grams.

Bulk density

Bulk density was determined by filling a 100 mL graduated cylinder with 25 mL of sample, weighing it, tapping it 10 times and then filling it to the 100 mL mark. Bulk density was calculated from sample weight and cylinder volume (Jan et al., 2015).

Antioxidant activities

The total phenolic content (TPC) extraction process of the samples was performed according to a method by Ghandehari Yazdi et al (2021) and the TPC analysis was determined using the Folin-Ciocalteau technique (Nordin et al., 2023). The *2,2-diphenyl-1-picrylhydrazyl* (DPPH) radical scavenging and ferric reducing antioxidant power (FRAP) assays were determined as reported by (Senevirathna et al. (2021).

Statistical analysis

All data were analyzed using the Minitab 21 statistical software (Minitab Inc.; State College, PA, USA). One-way analysis of variance (ANOVA), followed by Duncan's multiple range test at $p < 0.05$, was used to determine significance differences among means. Results were presented as mean ± SD.

Results and Discussion

Nutritional components of composite flours

The proximate composition analysis (Table 2) revealed that the addition of bambara bean flour significantly enhanced the nutritional profile of the samples. Formulation F3 had the highest contents of protein (16.52%), fat (5.22%), crude fiber (10.52%) and ash (2.90%), but the lowest carbohydrate content (51.72%), aligning with reported values for Bambara beans (Maphosa et al., 2022). In contrast, the F2 formulation had the highest carbohydrate content (81.00%) and lower protein and crude fiber contents, consistent with barley's role as a complex carbohydrate source rich in beta-glucan (Kaur et al., 2024). The F5 and F7 formulations had a balanced nutritional profile, with F5 containing elevated levels of protein (15.69%), fat (5.52%), crude fiber (5.40%) and ash (1.83%). Bambara bean flour increased the contents of protein, crude fiber, ash and fat (Ramashia et al., 2024), while barley flour raised carbohydrate levels. Significant differences were observed in all proximate parameters except moisture content 10.22 to 13.11%. Bambara flour (F3) had a moisture content of 13.11%, significantly higher than the other samples. A high level of moisture content can facilitate microbial proliferation and enzymatic activity, resulting in deterioration andthe generation of undesirable flavors and aromas, hence affecting the safety and shortening the shelf stability of the flour (Dzandu et al., 2023)

The color analysis (Table 2) revealed that the L* values were in the range 83.20 –93.38, the a* values were in the range 0.30–0.94 and the b* values were in the range 6.40–89.38. Barley flour (F2) had the highest L* and whiteness index values, while bambara bean flour (F3) had the lowest values. Incorporating Bambara bean flour significantly reduced the L* value in the blends (F5, F6, and F7) from 91.39 to 89.16, aligning with findings for bambara bean flour fortification of dark flour-based products (Mashau et al., 2022). In addition, the a* values decreased significantly from 0.94 to 0.30 in these blends, indicating darker coloration, while there was no significant increase in any of the b* values. Chroma, representing color intensity, decreased with the addition of barley (F4) and reached its lowest value in the F6 formulation, due to barley's lighter color resulting from pearling, which removes darker layers (Zheng et al., 2023). The F5 formulation had the lowest whiteness index (86.62), which was the darkest among the samples, likely due to the browning reactions of the broken rice during the milling process (Bruce et al., 2020).

The a_w (Table 2) measures the energy state of water in a food system, reflecting the extent to which water is bound within the food (Taoukis and Richardson, 2020). Most bacteria grow at $a_w \geq 0.91$, while fungi can grow at a_w values as low as 0.6, so maintaining a low a_w is essential for shelf stability, as water promotes chemical and microbial degradation in foods (Nevara et al., 2019). In the current study, the flour a_w was in the range 0.39–0.72, with F3 having the highest value (0.72) and F2 the lowest (0.39). All values were below the threshold for microbial growth (0.91), indicating good storage stability and potential for extended shelf life.

Table 2 Chemical composition of different flours and blends

Parameter	Formulation (see Table 1)						
	F1	F2	F3	F4	F5	F6	F7
Moisture content (%)	10.86±0.12^{c}	10.22±0.17^{d}	13.11±0.04^{a}	10.8±0.25^{c}	11.95±0.14^{b}	10.59±0.32^{cd}	10.68±0.25^{cd}
Fat (%)	1.68±0.07^{e}	1.80±0.09^{e}	5.22±0.10^{b}	2.59±0.14^{d}	5.52±0.20^{ab}	5.86±0.11^{a}	4.46±0.18^{c}
Protein (%)	11.40±0.15^{e}	5.72±0.10^{g}	16.52±0.06^{a}	8.80±0.14^{f}	15.69±0.17^{b}	14.11±0.15^{c}	12.04±0.19^{d}
Ash (%)	0.63±0.14^{g}	0.79±0.04^{f}	2.90±0.06^{a}	0.94±0.00^{e}	1.83±0.02^{c}	2.20±0.00^{b}	1.44±0.01^{d}
Crude fiber (%)	0.22±0.13^{d}	0.45±0.06^{d}	10.52±0.17^{a}	0.41±0.10^{d}	5.40±0.06^{b}	5.60±0.11^{b}	2.94±0.07^{c}
Carbohydrate (%)	75.22±0.08^{c}	81.00±0.26^{a}	51.72±0.13^{g}	76.45±0.45^{b}	59.61±0.06^{f}	61.64±0.44^{e}	68.45±0.25^{d}
L*	91.44±0.38^{b}	92.83±0.14^{a}	83.20±0.01^{e}	93.38±0.15^{a}	89.16±0.04^{d}	90.62±0.43^{c}	91.24±0.09^{bc}
a*	0.64±0.13^{b}	0.92±0.07^{a}	0.35±0.02^{c}	0.94±0.01^{a}	0.30±0.05^{c}	0.62±0.06^{b}	0.65±0.12^{b}
b*	7.24±0.25^{bc}	6.40±0.29^{c}	8.38±0.03^{a}	6.87±0.27^{c}	7.83±0.05^{ab}	7.20±0.25^{bc}	7.70±0.30^{ab}
Hue	1.48±0.01^{b}	1.43±0.00^{c}	1.53±0.00^{a}	1.43±0.01^{c}	1.53±0.00^{a}	1.48±0.01^{b}	1.49±0.01^{b}
Chroma	7.30±0.25^{c}	6.45±0.29^{e}	8.38±0.01^{a}	6.77±0.27^{de}	7.84±0.05^{b}	5.86±0.25^{f}	7.73±0.23^{b}
Whiteness index	88.77±0.29^{b}	90.34±0.26^{a}	81.22±0.08^{d}	90.53±0.23^{a}	86.62±0.05^{c}	88.16±0.28^{b}	88.31±0.23^{b}
Water activity	0.45±0.00^{e}	0.39±0.00^{g}	0.72±0.01^{a}	0.43±0.00^{f}	0.63±0.00^{b}	0.55±0.00^{c}	0.51±0.00^{d}
Amylose (%)	17.28±0.04^{d}	21.04±0.07^{a}	15.98±0.09^{e}	19.12±0.06^{b}	18.45±0.08^{c}	19.24±0.04^{b}	19.22±0.08^{b}
Amylopectin (%)	61.38±0.14^{a}	54.74±0.02^{b}	26.84±0.10^{g}	52.38±0.15^{c}	42.82±0.03^{e}	38.75±0.07^{f}	44.42±0.03^{d}
Starch (%)	78.66±0.10^{a}	75.78±0.08^{b}	42.82±0.07^{g}	71.50±0.11^{c}	61.27±0.07^{e}	57.99±0.11^{f}	63.64±0.05^{d}
Insoluble DF (%)	3.37±0.04^{g}	8.47±0.05^{d}	14.74±0.04^{a}	5.90±0.09^{f}	9.06±0.05^{c}	11.61±0.07^{b}	7.49±0.08^{e}
Soluble DF (%)	1.54±0.01^{d}	2.16±0.04^{a}	1.62±0.03^{cd}	1.87±0.07^{b}	1.56±0.06^{d}	1.88±0.07^{b}	1.72±0.04^{c}
Total DF (%)	4.91±0.03^{f}	10.63±0.01^{c}	16.36±0.01^{a}	7.77±0.04^{e}	10.62±0.06^{c}	13.49±0.09^{b}	9.21±0.09^{d}

DF = dietary fiber. Treatment details are shown in Table 1. Values (mean ± SD) within the same row followed by different lowercase superscript letters are significantly different ($p < 0.05$).

Despite the notably high a_w value for F3 (0.72) value, the microbial proliferation remained within crucial thresholds ($a_{w \leq}$0.91). An extended shelf life can be achieved by utilizing appropriate packaging and storage conditions, including the use of oxygen-barrier materials and low-temperature storage, which also minimize lipid oxidation (Hedegaard and Skibsted, 2024). The amylose content was in the range 15.98 –21.04%, with F2 having the highest value and F3 the lowest. Higher amylose contents are linked to greater gel strength and retrogradation. This occurs because of the abilities of amylose chains to form stable, compact network structures during retrogradation, which results in increased rigidity and elasticity of the gel (Geng et al., 2026). Thus, the high amylose content in F2 may produce firmer textures, as amylose facilitates amylopectin crystallization (Koekuyt and Marangoni, 2024). The amylopectin content was in the range from 26.84% (F3) to 61.38% (F1), which may have resulted in softer, moister products than those made from F3.

Food is classified as a source of fiber when it contains at least 3 g of dietary fiber per 100 g and it is considered a high-fiber food if it has 6 g or more per 100 g (Food and Agriculture Organization and World Health Organization, 2013). Based on Table 2, only F1 could be classified as a source of dietary fiber, while the other formulations would be categorized as high-fiber foods. Incorporating bambara bean flour in the F5 and F6 formulations significantly increased the insoluble dietary fiber (IDF) to 9.06% and 11.61%, respectively, and the TDF contents to 10.62% and 13.49%, respectively. Maphosa et al. (2022) reported that bambara bean varieties contained 10–16 g IDF/100 g. Thus, the addition of bambara bean flour directly increased the insoluble fiber content of the blends. Insoluble dietary fiber (IDF) mitigates gastrointestinal disorders, while the primary role of SDF is to inhibit the speed of digestion in the intestine, resulting in prolonged feelings of fullness and a reduced rate of blood glucose elevation (Nugraheni et al., 2022).

Particle size

Table 3 presents the particle size and functional properties of the composite flour blends, while their particle size distribution patterns are shown in Fig. 1. The F3 formulation had the largest particles (D10 =20.05 µm; D50 = 110.60 µm; D90 = 485.21 µm) due to its fibrous, protein-rich composition, resulting in a reduced surface area for water absorption. D50 is a key indicator of hydration and mixing, with smaller values promoting faster hydration and improved dough formation (Bressiani et al., 2019). The F6 formulation had the lowest D90 values (365.91 µm) with greater uniformity. In comparison, the F2 formulation had the lowest diameter (4.16 µm), indicating a homogeneous distribution that enhanced stability and water absorption (Kraithong et al., 2018).

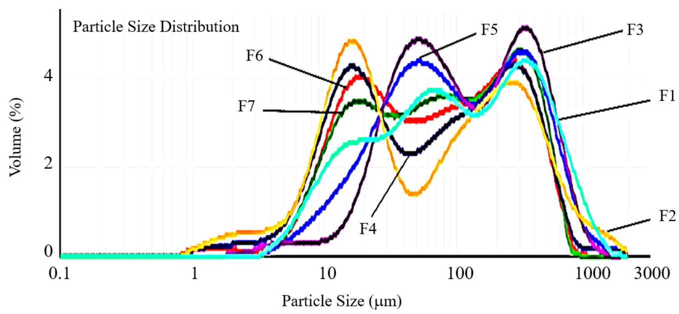

Fig. 1 Particle size distribution of composite flour blends (see Table 1 for F1 – F7 definitions).

Table 3 Particle size, functional properties and antioxidant activities of composite flour blends (see Table 1 for F1–F7 definitions).

Parameter	Formulation (see Table 1)						
	F1	F2	F3	F4	F5	F6	F7
D10 (µm)	13.45±0.29^{c}	8.62±0.04^{g}	25.05±0.15^{a}	9.67±0.29^{f}	18.85±0.10^{b}	11.66±0.08^{e}	12.39±0.02^{d}
D50 (µm)	101.70±0.05^{b}	63.85±0.18^{g}	110.60±0.54^{a}	67.53±0.51^{f}	98.93±0.54^{c}	70.59±0.53^{e}	79.85±0.51^{d}
D90 (µm)	534.16±0.17^{a}	447.69±0.29^{d}	485.21±0.20^{b}	383.83±0.09^{f}	475.91±0.57^{c}	365.91±0.21^{g}	385.25±0.50^{e}
Span	5.12±0.00^{c}	4.16±0.02^{f}	10.52±0.02^{a}	5.54±0.04^{b}	4.62±0.02^{e}	5.02±0.04^{d}	4.67±0.04^{e}
WAI (g/g)	2.20±0.02^{bc}	2.24±0.00^{bc}	2.31±0.15^{a}	2.08±0.02^{d}	2.27±0.03^{b}	2.08±0.03^{d}	2.03±0.05^{e}
WSI (%)	2.41±0.05^{g}	7.26±0.04^{e}	1.56±0.26^{a}	5.79±0.08^{f}	8.08±0.13^{d}	11.10±0.23^{b}	10.36±0.22^{c}
SP (g/g)	10.78±0.12^{cd}	10.59±0.15^{cd}	12.86±0.17^{a}	10.19±0.16^{d}	12.72±0.15^{ab}	11.59±0.14^{bc}	11.29±0.12^{cd}
BD (g/ml)	0.57±0.01^{a}	0.38±0.00^{e}	0.51±0.01b	0.46±0.00^{c}	0.55±0.00^{a}	0.42±0.01^{d}	0.49±0.00^{b}
TPC (mg GAE/g)	2.57±0.08^{e}	3.86±0.04^{cd}	8.15±0.06^{a}	3.45±0.18^{d}	6.26±0.14^{b}	6.67±0.14^{b}	4.69±0.13^{c}
DPPH (%RSA)	10.76±0.10^{d}	23.43±0.17^{b}	78.51±0.18^{a}	19.26±0.17^{e}	19.32±0.14^{e}	23.08±0.23^{g}	22.44±0.21^{f}
FRAP (µM TE/g)	3.81±0.02^{e}	4.49±0.13^{c}	6.62±0.12^{a}	4.65±0.17c	4.03±0.04^{d}	5.16±0.05^{b}	4.31±0.18c

WAI = water absorption index, WSI =water solubility index, SP = swelling power, BD =bulk density, TPC= total phenolic content; GAE = gallic acid equivalents; DPPH =*2,2-diphenyl-1-picrylhydrazyl; RSA = radical scavenging activity; FRAP* = ferric-reducing antioxidant power’ TE = trolox equivalent.

Values (mean ± SD) within the same row followed by different lowercase superscripts are significantly different ($p < 0.05$).

The WSI reflects the starch swelling capacity in excess water, while the WSI indicates polysaccharide release (Yousf et al., 2017). The composite flours had WAI and WSI values in the ranges 2.01–2.31 g/g and 1.56–11.10%, respectively, with significant differences. The F3 formulation had the highest WAI (2.31 g/g) due to its high protein and fiber content (Ramashia et al., 2024), while the F5 formulation also had a high WAI (2.27 g/g) from the contribution of Bambara. F7 had the lowest WAI (2.01 g/g), suggesting that combining the three flours might have reduced the water uptake due to component interactions that hindered gelatinization. The protein matrix in Bambara (Ogundele et al., 2017) and polysaccharides in barley influence these interactions, affecting absorption and gelatinization. The F6 formulation had the highest WSI (11.10%), attributed to synergistic interactions between the Bambara bean protein matrix and starch granules. The β-glucan in the barley further enhanced the WSI when blended with Bambara bean flour (F4, F6, and F7) at 5.79%, 11.10% and 10.36%, respectively. The barley soluble fiber dissolves in water, raising the WSI, which may have reduced the gelation capacity and batter viscosity, impacting texture and consistency. The swelling power of a flour quantifies the capacity of the starch granules in the flour to absorb water and expand when heated (Jiaet al., 2023). The F3 and F5 formulations had higher swelling power values of 12.86 g/g and 12.72 g/g, respectively, than the other formulations because Bambara bean flour has a high protein content, which enhances its swelling power and water absorption (Adeleke et al., 2018). The F2 formulation had the lowest bulk density (0.38 g/mL), indicating a more porous structure, which aligned with Li et al. (2021)who suggested a relationship between decreased bulk density and increased porosity in food products, since a decreased bulk density value signifies an increased presence of air spaces or pores within the material.

Sample F3 had the highest TPC (8.15 mg gallic acid equivalent/g), as shown in Table 3. Notably, bambara beans are abundant in hydroxycinnamic acids (chlorogenic and caffeic acids) and flavonoids, which contain many hydroxyl groups that serve as reactive sites for antioxidant activity (Oyeyinka et al., 2021). Phenolic compounds produce antioxidant activity through multiple mechanisms, such as donating hydrogen atoms to neutralize free radicals, chelating pro-oxidant metal ions and directly scavenging reactive oxygen species through electron transfer reactions (Shahidi and Ambigaipalan, 2015; Tungmunnithum et al., 2018). While the incorporation of broken rice and barley flour (F4) reduced the TPC due to its lower phenolic concentration, blends with bambara (F5, F6, F7) had greater TPC values than F4 (Yang et al., 2021). A strong positive correlation was observed between the TPC and antioxidant activity, as evaluated by DPPH radical scavenging activity (RSA) and ferric reducing antioxidant power (FRAP). F1 had the lowest results (10.76% RSA, 3.81 µM Trolox Equivalent (TE)/g), signifying a decreased antioxidant ability, whereas F3 had the greatest RSA (78.51%) and FRAP (6.62 µM TE/g). The DPPH test evaluates the capacity of phenolic compounds to donate hydrogen atoms or electrons to stabilize the DPPH radical, whereas FRAP assesses the reducing power by measuring electron donation to ferric ions (Fe^{3+}), therefore converting them to ferrous ions (Fe^{2+}) (Kedare and Singh, 2011; Apak et al., 2016).

The TPC, RSA and FRAP values were higher in the barley-Bambara blend (F5) compared to F4, attributable to synergistic interactions wherein phenolic compounds from diverse sources enhance each other's bioavailability and antioxidant effectiveness through interaction mechanisms, including the regeneration of oxidized antioxidants and complementary radical scavenging pathways (Mashau et al., 2022)

Fourier transform infrared spectroscopy.

FTIR spectroscopy was used to measure the short-range molecular order of the starch granules and to identify specific functional groups. Based on Fig. 2, there were similarities among the FTIR spectra of the seven composite flours. The mid-infrared spectra could be categorized into four distinct areas corresponding to the different molecular vibrations. Both protein and starch molecules had O–H stretching vibrations in the first region (3000–3800 cm^{-1}), with broad peaks indicating the stretching of the hydroxyl group.

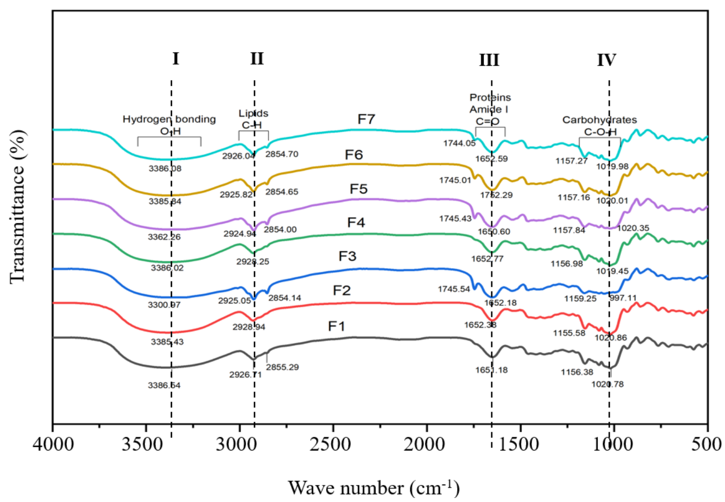

Fig. 2 Fourier transform infrared spectra of composite flour blends (see Table 1 for F1–F7 definitions).

Band shifts indicated that hydrogen bonding played a role in the molecular interactions between protein and starch, while other characteristics suggested changes in intramolecular or intermolecular hydrogen bonding. The density and strength of hydrogen bonds increase with decreasing wavenumbers (Sutrisno et al., 2024). Lipid components, specifically C–H, asymmetric $–CH_2$ and symmetric $–CH_2$ stretching vibrations, were linked to the second region (2928 cm^{-1} and 2854 cm^{-1}) (Candoğan et al., 2021). The third region contained amide I (1631–1634 cm^{-1}) and amide II (1534–1539 cm^{-1}) bands, coming from C=O, N–H and C–N stretching and from N–H bending in combination with C–N stretching, respectively. These bands, resulting from the vibrations of the peptide backbone and isopeptide linkages, represent the structural configurations of proteins. After adding Bambara bean flour, the amide band intensity increased, suggesting that the composite flours had a higher protein content. F1, F2 and F4 did not have the peak at 1745 cm^{-1} (Sutrisno et al., 2024). Starch-specific spectral features, specifically C–O and C–C stretching vibrations, were represented by the fourth region (1200–800 cm^{-1}). In this starch region, formulations that combined barley flour and broken rice flour displayed increased peak intensities. Amylose molecules may reduce the molecular short-range order by preventing the formation of double-helical arrangements (Zhang et al., 2022).

The enhancement of amide I/II band intensity and alterations in the extensive O–H stretching area in the bambara-enriched blends signified an elevated protein content and a changed hydrogen-bonding environment. The shift of the amide I band from 1631-1634 cm^{-1} indicated alterations in the protein secondary structure, specifically the β-sheet and random coil conformations, which may have disrupted the starch molecular organization (Kong and Yu, 2007). Proteins and dietary fibers may bind to starch surfaces through electrostatic interactions and hydrogen bonding between amino acid residues and the hydroxyl groups of glucose units (Zhou et al., 2024), potentially restricting the reassociation of amylose/amylopectin chains and modifying hydrogen-bond networks essential for recrystallization after cooling (retrogradation). Legume proteins from Bambara beans produce a physical barrier surrounding starch granules, restricting water mobility and reducing the conformational flexibility required for double helix formation during retrogradation (Roman et al., 2025). Thus, interactions between protein-starch and fiber-starch reduce the mobility and alignment of starch chains required for crystal formation, resulting in reduced setback and enhanced paste stability (Shao et al., 2023; Scott and Awika, 2023). The wavenumber shift in the O–H stretching area, from 3400 to 3300 cm^{-1}, signified enhanced hydrogen bonding networks and corresponding to increased molecular interactions between starch and non-starch components (Koshenaj and Ferrari, 2024). The FTIR-detected band shifts were used as indicators of modified hydrogen bonding, which corresponded to variations in the pasting and gelation behavior determined using the RVA (Roman et al., 2025).

Samples F3 and F7 had broadening and shifts in the O–H stretching region of the FTIR spectra. These spectrum alterations signified modified hydrogen bonding, which decreased the capacity of the starch chains to reassemble after cooling. Consequently, both formulations had reduced setback viscosity and enhanced paste stability. This process aligned with other research indicating that alterations in hydrogen bonding within starch systems resulted in reduced retrogradation and enhanced freeze-thaw stability (Wang et al., 2021; Lin et al., 2023).

X-ray diffraction

Often, the XRD pattern is utilized to ascertain the crystalline structure of flours. Fig. 3a and 3b present the XRD patterns of the flour mixtures (F1–F7). The A-type crystalline peaks at approximately 15°, 17°, 18° and 23° (2θ) in the XRD analysis (F1–F7) were characteristic of cereal starches (Li et al., 2022), with the peaks at 15° and 23° corresponding to the pasting and gelatinization temperatures. F1 had the highest relative crystallinity (RC) at 45.57%, F3 had the lowest at 22.31% and F5 had an intermediate RC of 32.30%. Since amylose breaks down amylopectin double helices and crystalline order, RC was inversely correlated with the amylose content (Teng et al., 2017). The high contents of protein (18–25%) and fiber (6–12%) in the Bambara bean flour interfered with starch crystallinity (Oyeyinka et al., 2017), resulting in more amorphous regions that improved water absorption and swelling and lowered the gelatinization temperature. While a low RC reflects disrupted molecular order, it also indicates higher reactivity and digestibility (Chinma et al., 2021), as well as promoting water infiltration, rapid swelling and a lower gelatinization energy (Liu et al., 2024). On the other hand, a high RC indicates greater structural stability (Li et al., 2022). Low-crystallinity flours are better suited for quick cooking products, offering enhanced solubility, water absorption and sensory quality, whereas high-crystallinity flours preserve firm textures in pasta and extruded snacks (Yan et al., 2025).

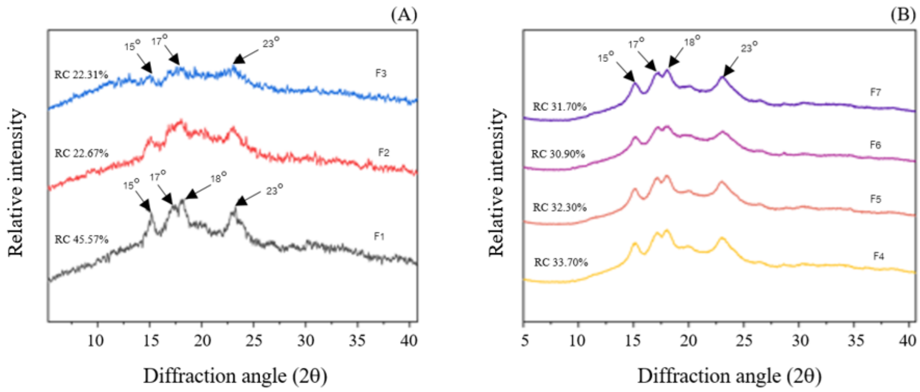

Fig. 3 X-ray diffraction pattern of: (A) raw material flour; (B) flour blends (see Table 1 for F1–F7 definitions).

Sample F3, which contained the highest proportion of Bambara flour, had the lowest relative crystallinity (22.31%) in the X-ray diffraction results. Commonly, this reduction in crystallinity is associated with a more amorphous starch matrix and greater disruption of the double helical regions, with such structural changes promoting water penetration during heating and limiting the reordering of starch chains during cooling (Chinma et al., 2021). These structural features help to explain the lower setback viscosity observed in F3 (358.67 cP), as shown in Table 4, compared with the higher setback values of the rice-dominant samples F1, F4, F5 and F7, at 2,390.70 cP, 1,992.00 cP, 1,399.30 cP and 1,809.70 cP, respectively. Similar relationships between low crystallinity and reduced retrogradation have been well documented in the literature (Wang et al., 2021; Tingting Kou et al., 2022).

Pasting properties

The RVA results for the different flours and mixtures are summarized in Table 4 and Fig.4 illustrates the pasting curves of the composite flour blends. The final viscosity reflects a substance's ability to form a thick, viscous paste (Kaushal et al., 2012). The setback viscosity (SV) denotes the viscosity recovery that takes place following the cooling of a heated starch solution and reflects the tendency of the starch to retrograde as the cooked starch paste cool down. The final viscosity (FV) and the setback viscosity (SV) values of several flours varied considerably, ranging from 1,127 cP (F3) to 3,899 cP (F1) and from 358 cP (F3) to 2,390 cP (F1), respectively (Table 4).

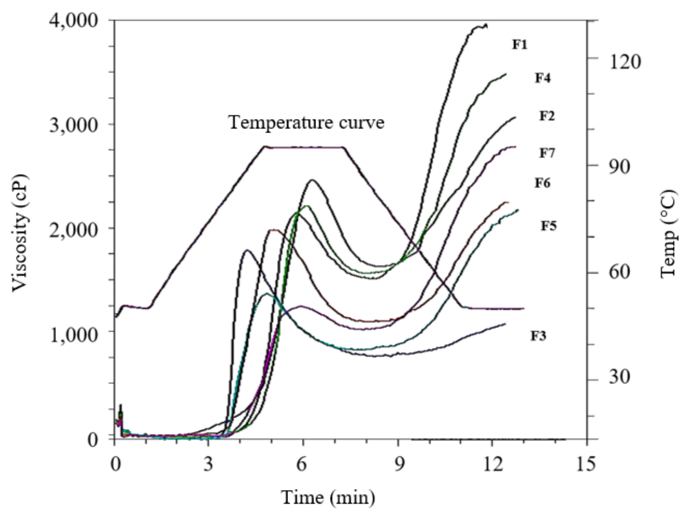

Fig. 4 Pasting curves of composite flour blends (see Table 1 for F1–F7 definitions).

Table 4 Pasting properties of composite flour blend (see Table 1 for F1–F7 definitions).

Sample code	F1	F2	F3	F4	F5	F6	F7
PV (cP)	1,976.80±73.40^{b}	2,303.94±81.33^{a}	1,644.70±90.20^{c}	2,062.00±85.40^{b}	1,313.20±64.30^{d}	1,941.10±97.30^{b}	1,181.58±72.74^{d}
TV (cP)	1,508.70±98.30^{a}	1,494.00±90.38^{a}	765.67±105.86^{c}	1,524.70±78.90^{a}	883.30±82.70^{bc}	1,071.00±49.00^{b}	1,035.67±87.10^{b}
BV (cP)	594.30±27.60^{cd}	847.70±47.40^{b}	981.00±44.50^{a}	669.00±60.00^{c}	513.70±69.20^{d}	994.00±65.00^{a}	221.22±56.66^{e}
FV (cP)	3,899.33±54.47^{a}	3,050.00±53.00^{c}	1,127.33±95.03^{e}	3,516.70±97.30^{b}	2,282.70±44.67^{d}	2,309.00±55.00^{d}	2,845.30±48.40^{c}
SV (cP)	2,390.70±72.70^{a}	1,556.00±88.52^{d}	358.67±98.02^{f}	1,992.00±31.80^{b}	1,399.30±52.62^{d}	1,238.00±59.00^{e}	1,809.70±66.50^{c}
Peak time (min)	5.84±0.07^{b}	6.18±0.11^{a}	4.20±0.07^{d}	6.12±0.14^{ab}	4.93±0.07^{c}	5.03±0.03^{c}	5.93±0.07^{b}
Pasting temp (°C)	83.65±0.07^{b}	67.47±0.11^{d}	79.30±0.07^{c}	88.77±0.14^{a}	79.57±0.07^{c}	81.55±0.03^{bc}	83.68±0.07^{b}

PV = peak viscosity; TV = trough viscosity; BV = breakdown viscosity; FV = final viscosity; SV = setback viscosity.

Values (mean ± SD) within the same row followed by different lowercase superscript letters are significantly different ($p < 0.05$)

Notably, the SV diminished with the incorporation of Bambara bean flour in the mixtures, signifying the bean flour's reduced propensity for retrogradation. A reduced inclination to retrograde is beneficial in culinary preparations, such as sauces and soups, which experience precipitation and viscosity loss (Liu et al., 2020). The reduced setback and breakdown viscosities of the flour indicate a significant resistance to retrogradation, leading to the development of a consistent paste, which is a crucial characteristic in porridges (Kaushal et al., 2012).

The lowest temperature at which flour can gelatinize is known as the pasting temperature (PT). F2 had the lowest PT (67.47°C) because of its high protein and fiber contents that disrupted gelatinization, while F4 had the highest PT (88.77°C), probably because its starch-protein interactions improved the thermal stability. According to Wang et al. (2016), formulations containing broken rice typically had higher PT values, which was consistent with the rice amylose content raising the gelatinization temperature and indicating greater resistance to swelling. In the current study, the β-glucan content of the barley was responsible for the highest peak viscosity (PV) in F2 (2,303.94 cP), while the dilution from three-flour blending resulted in the lowest PV in F7 (1,181.58 cP). F4 had the highest trough viscosity, indicating paste stability, due to synergistic water absorption and reduced solubility, while F3 had the lowest trough viscosity, where starch hydration was restricted by the protein matrix of the bambara bean flour (Ogundele et al., 2017).

Granule disintegration is reflected in the breakdown viscosity (BV), where a lower BV indicates higher thermal and shear stability (Yadav et al., 2022). In the current study, F6 had the highest BV, while F7 had the lowest. Broken rice flour improved the gelatinization stability by lowering the BV (Yang et al., 2021). The ranges for the FV and SV were 1127–3899 cP and 358–2390 cP, respectively. For products such as sauces, soups and porridges that require paste stability at low temperatures, the addition of bambara bean flour decreased the SV, indicating a lower retrogradation potential (Kaushal et al., 2012).

Formulations F3 and F5, which incorporated higher concentrations of Bambara flour components, such as protein and soluble fiber (Table 2), had reduced amylose availability, which resulted in reduced pasting temperatures and decreased setback viscosities. Their peak viscosities were 1,644.70 cP for F3 and 1,313.20 cP for F5. Amylose dilution correlates with decreased chain alignment during cooling and rapid viscosity development, providing a functional benefit in instant or quick-cooking products (Jia et al., 2023) The higher soluble fiber content in sample F3 improved water absorption and swelling power, resulting in a moderate peak viscosity and a stable hot-paste profile. These attributes are advantageous in foods, such as porridges and beverages, where a smooth texture and moisture retention are desirable characteristics (Maphosa et al., 2022).

The spectral results for sample F7 indicated the formation of lipid, protein, and starch complexes, which mitigated amylose leaching during heating. The F7 formulation had a moderate peak viscosity (1,181.58 cP) and a low breakdown value. These complexes enhance thermal stability and are advantageous for products processed at high temperatures such as retorted foods and extruded products (Shao et al., 2023; Scott and Awika, 2023). On the other hand, sample F1, characterized by a majority of the broken rice flour, exhibited higher crystallinity and produced more robust gel formations during cooling. The SV was the highest among all the formulations (2,390.70 cP). These attributes would be beneficial in structured food products, such as noodles and extruded snacks, where hardness and shape preservation are crucial characteristics (Kraithong et al., 2018).

Conclusion

The incorporation of bambara bean and barley flours into broken rice flour significantly increased the contents of protein, dietary fiber, fat and total phenolics, while decreasing the levels of starch and amylose. Blends containing higher Bambara content had a larger particle size, improved water absorption and greater antioxidant activity. Based on the analysis of the pasting properties, there was a decrease in the breakdown and setback viscosities, indicating enhanced heat stability and a reduced tendency for retrogradation. Furthermore, the FTIR and XRD measurements confirmed the reduction in crystallinity and the altered hydrogen bonding configurations. This study addressed the stated research gap by demonstrating that the tested novel triple-flour combination produced synergistic functional and nutritional benefits that exceeded those of previously reported binary blends, while also increasing the value of broken rice, a previously underutilized milling by-product. The various pasting profiles should facilitate specific industrial applications: high-crystallinity formulations (F1, F4) are suitable for structured products such as noodles and extruded snacks; low-setback formulations (F3, F5) are suitable for sauces, soups and instant beverages that need a smooth texture and storage stability; and intermediate blends (F6, F7) are suitable for baked applications. The high antioxidant capacity of the Bambara-rich blends indicated that they are suitable as functional materials for health-focused products, which would decrease agricultural waste by utilizing broken rice and enhance food security through crop diversification. Future research should focus on sensory evaluation and consumer acceptability studies, as well as the optimization of pilot-scale processing (extrusion, baking, noodle-making), glycemic index assessment and the investigation of pre-processing treatments to enhance product functionality. These findings should underpin the development of value-added, fiber-rich and healthier food products from an underutilized crop.

Conflict of Interest

The authors declare that there are no conflicts of interest.

Acknowledgements

The Southeast Asian Regional Center for Graduate Study and Research in Agriculture (SEARCA) provided funding (Grant Number GBG23-1056) and Padi Beras Nasional Berhad (BERNAS) Malaysia supplied the rice samples used in this study.

References

Adeleke, O.R., Adiamo, O.Q., Fawale, O.S. 2018. Nutritional, physicochemical and functional properties of protein concentrate and isolate of newly-developed Bambara groundnut (*Vigna subterrenea* L.) cultivars. Food Sci. Nutr. 6: 229–242. doi.org/10.1002/fsn3.552

Apak, R., Özyürek, M., Güçlü, K., Çapanoğlu, E. 2016. Antioxidant activity / capacity measurement: 1. Classification, physicochemical principles, mechanisms and electron transfer (ET)-based assays. J. Agric. Food Chem. 34: 997–1027. doi.org/10.1021/acs.jafc.5b04739

Ariyantoro, A.R., Praseptiangga, D., Anam, C., et al. 2021. Physical, chemical, physicochemical and sensory properties of analog rice based on purple sweet potato flour (*Ipomoea batatas* L.) and bambara groundnut flour (*Vigna subterranea* L.). IOP Conf. Ser. Earth Environ. Sci. 828: 012030. doi.org/10.1088/1755-1315/828/1/012030

Bressiani, J., Oro, T., Da Silva, P.M.L., Montenegro, F.M., Bertolin, T.E., Gutkoski, L.C., Gularte, M.A. 2019. Influence of milling whole wheat grains and particle size on thermo-mechanical properties of flour using Mixolab. Czech J. Food Sci. 37: 276–284. doi.org/10.17221/239/2018-CJFS

Bruce, R.M., Atungulu, G.G., Sadaka, S. 2020. Impacts of size fractionation, commingling and drying temperature on physical and pasting properties of broken rice kernels. Cereal Chem. 97: 256–269. doi.org/10.1002/cche.10241

Candoğan, K., Altuntas, E.G., İğci, N. 2021. Authentication and quality assessment of meat products by Fourier-transform infrared (FTIR) spectroscopy. Food Eng. Rev. 13: 66–91. doi.org/10.1007/s12393-020-09251-y

Chinma, C.E., Abu, J.O., Asikwe, B.N., Sunday, T., Adebo, O.A. 2021. Effect of germination on the physicochemical, nutritional, functional, thermal properties and in vitro digestibility of Bambara groundnut flours. LWT, 140: 110749. doi.org/10.1016/j.lwt.2020.110749

Dzandu, B., Kumi, S., Asirifi-addo, T. 2023. Quality assessment of gluten-free cookies from rice and Bambara groundnut flour. CyTA J. Food. 21: 258–268. doi.org/10.1080/19476337.2023.2190792

Food and Agriculture Organization and World Health Organization. 2013. Codex guideline for use of nutrition and health claims - CAC/GL 23-1997. Codex Alimentarius Commission 23: 1–8. http://www.fao.org/ag/humannutrition/3244409f5545b8abe9a0c3baf01a4502ac36e4.pdf

Geng, D.H., Tang, N., Zhang, N., Wang, K., Asiamah, E., Cheng, Y., Zhao, X. 2026. Effect of starch chain structures on the order, strength, and digestibility of retrograded starch structures: A review. Carbohydr. Polym. 375: 124796. doi.org/10.1016/j.carbpol.2025.124796

Ghandehari Yazdi, A.P., Barzegar, M., Sahari, M.A., Gavlighi, H.A. 2021. Encapsulation of pistachio green hull phenolic compounds by spray drying. J. Agric. Sci. Technol. 23: 51–64.

Hasmadi, M., Ronie, M.E. 2022. Factors affecting the properties of rice flour: A review. Food Research 6:1–12. doi.org/10.26656/fr.2017.6(6).531

Hedegaard, R.V, Skibsted, L.H. 2024. Shelf-life of food powders. In: Bhandari, B., Bansal, N., Zhang, M., Schuck, P. (Eds.). Handbook of Food Powders: Chemistry and Technology, 2nd ed. Elsevier Ltd. Amsterdam, the Netherlands. pp. 335–354

Horwitz, W., Latimer, G.W. 2005. Official Methods of Analysis of AOAC International 18th ed. 2005. Association of Official Analytical Chemistry International. Rockville, MD, USA.

Lafont-Mendoza, J.J., Severiche-Sierra, C.A., Jaimes-Morales, J. 2018. Evaluation of the starch quantification methods of using factorial experiments. Int. J. Food Sci. 2018: 1–7.

Jan, S., Insha, S., Saxena, D.C., Rafiq, S.I. 2015. Effect of physical properties on flowability of commercial rice flour/powder for effective bulk handling. IJCA Proc. Int. Conf. Adv. Eng. Technol. 11: 1–5.

Jia, R., Cui, C., Gao, L., et al. 2023. A review of starch swelling behavior: Its mechanism, determination methods, influencing factors and influence on food quality. Carbohydr. Polym. 321: 121260. doi.org/10.1016/j.carbpol.2023.121260

Jozinović, A., Šubarić, D., Ačkar, Đ., Babić, J., Orkić, V., Guberac, S., Miličević, B. 2021. Food industry by-products as raw materials in the production of value-added corn snack products. Foods. 10: 946. doi.org/10.3390/foods10050946

Kaur, A., Purewal, S.S., Phimolsiripol, Y., Punia Bangar, S. 2024. Unraveling the hidden potential of barley (*Hordeum vulgare*): An important review. Plants. 13: 2421. doi.org/10.3390/plants13172421

Kaushal, P., Kumar, V., Sharma, H.K. 2012. Comparative study of physicochemical, functional, antinutritional and pasting properties of taro (*Colocasia esculenta*), rice (*Oryza sativa*) flour, pigeonpea (*Cajanus cajan*) flour and their blends. LWT - Food Sci. Technol. 48: 59–68. doi.org/10.1016/j.lwt.2012.02.028

Kedare, S.B., Singh, R.P. 2011. Genesis and development of DPPH method of antioxidant assay. J. Food Sci. Technol. 48: 412–422. doi.org/10.1007/s13197-011-0251-1

Kharat, S., Medina-Meza, I.G., Kowalski, R.J., Hosamani, A., Ramachandra, C.T., Hiregoudar, S., Ganjyal, G.M. 2019. Extrusion processing characteristics of whole grain flours of select major millets (foxtail, finger and pearl). Food Bioprod. Process. 114: 60–71. doi.org/10.1016/j.fbp.2018.07.002

Koekuyt, H.A., Marangoni, A.G. 2024. The solid state and nanostructure of starch: Effects on starch functionality. Crit. Rev. Food Sci. Nutr. doi.org/10.1080/10408398.2024.2388279

Kong, J., Yu, S. 2007. Fourier transform infrared spectroscopic analysis of protein secondary structures: Protein FTIR data analysis and band assignment. Acta Biochim. Biophys. Sin. 39: 549–559. doi.org/10.1111/j.1745-7270.2007.00320.x

Koshenaj, K., Ferrari, G. 2024. A comprehensive review on starch-based hydrogels: From tradition to innovation, opportunities and drawbacks. Polymers. 16: 1991. doi.org/10.3390/polym16141991

Kraithong, S., Lee, S., Rawdkuen, S. 2018. Physicochemical and functional properties of Thai organic rice flour. J. Cereal Sci. 79: 259–266. doi.org/10.1016/j.jcs.2017.10.015

Li, Q.Q., Chen, X., Bi, W.Y., Jiang, J.Y., Shi, T.Y. 2021. Research on determination method and influencing factors of porosity of wheat pile. Sci. Technol. Cereals Oils Foods. 29: 187–193. doi.org/10.16210/j.cnki.1007-7561.2021.01.025

Li, Y., Zhao, L., Lin, L., Li, E., Cao, Q., Wei, C. 2022. Relationships between X-ray diffraction peaks, molecular components and heat properties of C-type starches from different sweet potato varieties. Molecules. 27: 3385. doi.org/10.3390/molecules27113385

Lin, X., Zhang, X., Du, B., Xu, B. 2023. Morphological, structural, thermal, pasting and digestive properties of starches isolated from different varieties of rice: A systematic comparative study. Foods. 12: 4492. doi.org/10.3390/foods12244492

Liu, W., Zhang, M., Devahastin, S., Wang, W. 2020. Establishment of a hybrid drying strategy for instant cream mushroom soup based on starch retrogradation behavior. *Int.* J. Biol. Macromol. 147: 463–472. doi.org/10.1016/j.ijbiomac.2020.01.084

Liu, Y., Shen, W., Jin, W., Li, F., Chen, X., Jia, X., Cai, H. 2024. Physicochemical characterization of a composite flour: Blending purple sweet potato and rice flours. Food Chem. X. 22: 101493. doi.org/10.1016/j.fochx.2024.101493

Lukinac, J., Jukić, M. 2022. Barley in the production of cereal-based products. Plants. 11: 3519. doi.org/10.3390/plants11243519

Lv, Y., Ma, S., Yan, J., Sun, B., Wang, X. 2022. Effect of heat–moisture treatment on the physicochemical properties, structure, morphology and starch digestibility of highland barley (*Hordeum vulgare* L. var. *nudum* Hook. f) flour. Foods. 11: 3511. doi.org/10.3390/foods11213511

Maphosa, Y., Jideani, V.A., Maphosa, L. 2022. Bambara groundnut production, grain composition and nutritional value: Opportunities for improvements. J. Agric. Sci. 160: 448–458. doi.org/10.1017/S0021859622000521

Mashau, M.E., Mukwevho, T.A., Ramashia, S.E., Siwela, M. 2022. The influence of Bambara groundnut (*Vigna subterranean*) flour on the nutritional, physical and antioxidant properties of steamed bread. CyTA J. Food. 20: 259–270. doi.org/10.1080/19476337.2022.2130435

Mustapha, N.A., Yan, T.L., Ibadullah, W.Z.W., Shukri, R., Ibrahim, N.H. 2024. Microwave-and oven-heat moisture treatment of broken rice flour and the improvement in flat rice noodle quality. J. Adv. Res. Appl. Sci. Eng. Technol. 43: 33–44. doi.org/10.37934/araset.43.1.3344

Nevara, G.A., Yea, C.S., Karim, R., Muhammad, K., Mohd Ghazali, H. 2019. Effects of moist-heat treatments on color improvement, physicochemical, antioxidant and resistant starch properties of drum-dried purple sweet potato powder. J. Food Process Eng. 42: e12951. doi.org/10.1111/jfpe.12951

Nisha, R., Nickhil, C., Pandiarajan, T., Pandiselvam, R., Jithender, B., & Kothakota, A. 2023. Chemical, functional, rheological and structural properties of broken rice–barnyard millet–green gram grits blend for the production of extrudates. J. Food Process Eng. 46: 1–15. //doi.org/10.1111/jfpe.1432

Nordin, N.L., Sulaiman, R., Bakar, J., Noranizan, M.A. 2023. Comparison of phenolic and volatile compounds in MD2 pineapple peel and core. Foods. 12: 2233. doi.org/10.3390/foods12112233

Nugraheni, M., Purwanti, S., Ekawatiningsih, P. 2022. Chemical composition, glycaemic index and antidiabetic property of analogue rice made from composite tubers, germinated legumes and cereal flours. Int. Food Res. J. 29: 1304–1313. doi.org/10.47836/ifrj.29.6.07

Ogundele, O.M., Minnaar, A., Emmambux, M.N. 2017. Effects of micronisation and dehulling of pre-soaked bambara groundnut seeds on microstructure and functionality of the resulting flours. Food Chem. 214: 655–663. doi.org/10.1016/j.foodchem.2016.07.022

Okafor, J. N. C., Jideani, V. A., Meyer, M., & Le Roes-Hill, M. 2022. Bioactive components in Bambara groundnut (Vigna subterraenea (L.) Verdc) as a potential source of nutraceutical ingredients. Heliyon, 8: e09024. doi.org/10.1016/j.heliyon.2022.e09024

Oyeyinka, S.A., Abdulsalam, A.O., Ahmed El-Imam, A.M., et al. 2021. Total phenolic content, antioxidant, anti-inflammatory and anti-microbial potentials of Bambara groundnut (*Vigna subterranea* L.) seed extract. Br. Food J. 123: 3421–3435. doi.org/10.1108/BFJ-07-2020-0637

Oyeyinka, S.A., Singh, S., Amonsou, E.O. 2017. Physicochemical properties of starches extracted from bambara groundnut landraces. Starch. 69: 1600089. doi.org/10.1002/star.201600089

Palupi, N.S., Kusnandar, F., Lestari, O.A. 2015. Biological values of dried corn noodles substituted with heat moisture treated (HMT)-corn flour. J. Teknol. Ind. Pangan. 26: 9–16. doi.org/10.6066/jtip.2015.26.1.9

Ramashia, S.E., Sikhipha, R.C., Olamiti, G., Mashau, M.E. 2024. Nutritional, antioxidant and structural properties of rusk developed from wheat–Bambara groundnut (*Vigna subterranean*) flour. Legume Sci. 6: e70015. doi.org/10.1002/leg3.70015

Ren, Y., Linter, B. R., Linforth, R., & Foster, T. J. 2020. A comprehensive investigation of gluten free bread dough rheology, proving and baking performance and bread qualities by response surface design and principal component analysis. *Food and Function*, *11*: 5333–5345. doi.org/10.1039/d0fo00115e

Roman, L., Jim, L., Jakobsen, L.M.A., Corredig, M. 2025. The role of amylose content on the structure and rheological properties of pea protein-starch systems during pressurized hydrothermal processing. Food Hydrocoll. 160: 110830. doi.org/10.1016/j.foodhyd.2024.110830

Senevirathna, S. S. J., Ramli, N. S., Azman, E. M., Juhari, N. H., & Karim, R. (2021). Optimization of the drum drying parameters and citric acid level to produce purple sweet potato (*Ipomoea batatas* L.) powder using response surface methodology. *Foods*, *10*(6). https://doi.org/10.3390/foods10061378

Scott, G., Awika, J.M. 2023. Effect of protein-starch interactions on starch retrogradation and implications for food product quality. Compr. Rev. Food Sci. Food Saf. 22: 2081–2111. doi.org/10.1111/1541-4337.13141

Shahidi, F., Ambigaipalan, P. 2015. Phenolics and polyphenolics in foods, beveragesand spices: Antioxidant activity and health effects. J. Funct. Foods. 18: 820–897. doi.org/10.1016/j.jff.2015.06.018

Shao Y, Jiao R, Wu Y, Xu F, Li Y, Jiang Q, Zhang L, Mao L. 2023. Physicochemical and functional properties of the protein-starch interaction in Chinese yam. Food Sci. Nutr. 11: 1499–1506. doi.org/10.1002/fsn3.3189

Sutrisno, A., Suloi, A.N.F., Murtini, E.S., Bahmid, N.A. 2024. The effect of corn starch and transglutaminase on quality improvement of soybean-based analog rice. Future Foods. 10: 100407. doi.org/10.1016/j.fufo.2024.100407

Tan, B.L., Norhaizan, M.E. 2020. Rice By-products: Phytochemicals and Food Products Application. Springer. New York, NY, USA

Taoukis, P.S., Richardson, M. 2020. Principles of Intermediate - Moisture Foods and Related Technology. In: Barbosa-Cánovas, G.V., Fontana Jr, A.J., Schmidt, S.J. Labuza, T.P. (Eds.). *Water Activity in Foods: Fundamentals and Applications,* 2nd ed. Blackwell Publishing. pp. 385–424.

Teng, B., Zhang, Y., Du, S., Wu, J., Li, Z., Luo, Z., Yang, J. 2017. Crystalline, thermal and swelling properties of starches from single-segment substitution lines with different *Wx* alleles in rice (*Oryza sativa* L.). J. Sci. Food Agric. 97: 108–114. doi.org/10.1002/jsfa.7693

Thiranusornkij, L., Thamnarathip, P., Chandrachai, A., Kuakpetoon, D., Adisakwattana, S. 2019. Comparative studies on physicochemical properties, starch hydrolysis, predicted glycemic index of Hom Mali rice and Riceberry rice flour and their applications in bread. Food Chem. 283: 224–231. doi.org/10.1016/j.foodchem.2019.01.048

Tingting, K., Song, J., Mouquan, L., Guihong, F. 2022. Effect of amylose and crystallinity pattern on the gelatinization behavior of cross-linked starches. Polymers. 14: 2870.

Tungmunnithum, D., Thongboonyou, A., Pholboon, A. 2018. Flavonoids and other phenolic compounds from medicinal plants for pharmaceutical and medical aspects: An overview. Medicines. 5: 93. doi.org/10.3390/medicines5030093

Wang, L., Guo, J., Wang, R., Shen, C., Li, Y., Luo, X., Li, Y., Chen, Z. 2016. Studies on quality of potato flour blends with rice flour for making extruded noodles. Cereal Chem. 93: 593–598. doi.org/10.1094/CCHEM-05-16-0147-R

Wang, Y., Chen, L., Yang, T., Ma, Y., McClements, D.J., Ren, F., Tian, Y., Jin, Z. 2021. A review of structural transformations and properties changes in starch during thermal processing of foods. Food Hydrocoll. 113: 106543. doi.org/10.1016/j.foodhyd.2020.106543

Yadav, G.P., Dalbhagat, C.G., Mishra, H.N. 2022. Effects of extrusion process parameters on cooking characteristics and physicochemical, textural, thermal, pasting, microstructure and nutritional properties of millet-based extruded products: A review. J. Food Process Eng. 45: e14106. doi.org/10.1111/jfpe.14106

Yan, X., Tian, L., Xiao, H., et al. 2025. Heat-stable single-helical structures formed during the extrusion process play a key role in the cooking and texture qualities of rice noodles. Int. J. Biol. Macromol. 301: 140066. doi.org/10.1016/j.ijbiomac.2025.140066

Yang, X., Shi, H., Mi, X., Wang, L. 2021. Gelatinization and rheological properties of blend of defatted rice bran and broken rice. IOP Conf. Ser. Earth Environ. Sci. 792: 012002. doi.org/10.1088/1755-1315/792/1/012002

Yao, D.N., Kouassi, K.N., Erba, D., Scazzina, F., Pellegrini, N., Casiraghi, M.C. 2015. Nutritive evaluation of the bambara groundnut Ci12 landrace [*Vigna subterranea* (L.) Verdc. (Fabaceae)] produced in Côte d'Ivoire. Int. J. Mol. Sci. 16: 21428–21441. doi.org/10.3390/ijms160921428

Yousf, N., Nazir, F., Salim, R., Ahsan, H., Sirwal, A. 2017. Water solubility index and water absorption index of extruded product from rice and carrot blend. J. Pharmacogn. Phytochem. 6: 2165–2168.

Zeng, Y., Pu, X., Du, J., Yang, X., Li, X., Mandal, M. S. N., Yang, T., Yang, J. 2020. Molecular Mechanism of Functional Ingredients in Barley to Combat Human Chronic Diseases. *Oxid. Med. Cell. Longev*. 2020: 1–26. doi.org/10.1155/2020/3836172

Zhang, Z., Hu, Y., Zhao, J., Zhang, Y., Ying, Y., Xu, F., Bao, J. 2022. The role of different *Wx* and *BEIIb* allele combinations on fine structures and functional properties of indica rice starches. Carbohydr. Polym. 278: 118972. doi.org/10.1016/j.carbpol.2021.118972

Zheng, Q., Wang, Z., Xiong, F., Song, Y., Zhang, G. 2023. Effect of pearling on nutritional value of highland barley flour and processing characteristics of noodles. Food Chem. X. 17: 100596. doi.org/10.1016/j.fochx.2023.100596

Zhou, J., Zheng, S., Chen, Q., Wan, X., Du, J., Ding, W., Wang, X., Zhang, H. 2024. Effect of legume proteins on the structure and digestibility of wheat starch-lauric acid complexes. Food Chem. X. 24: 101891. doi.org/10.1016/j.fochx.2024.101891